P-Wave Morphological Variability Exacerbation Prior to Atrial Fibrillation Episodes

Maikel Noriega[1], Alba Martín-Yebra[2,1], Aleksei Savelev[3], Pyotr Platonov[3], Javier Marta[4], Monika Butkuviene[5], Juan Pablo Martínez[1], Pablo Laguna[1]

[1] BSICoS-I3A, Zaragoza University; CIBER-BBN, Zaragoza, Spain
[2] Aragonese Foundation for Research & Development , ARAID, Zaragoza, Spain
[3] Department of Cardiology, Clinical Sciences, Lund University, Lund, Sweden
[4] Instituto de Investigación Sanitaria Aragón (IIS Aragón), Zaragoza University, Zaragoza, Spain
[5] Biomedical Engineering Institute, Kaunas University of Technology, Kaunas, Lithuania

Abstract

This study analyzes the temporal evolution of the short-term P-wave morphological variability (PWMV) within the one-hour interval immediately preceding the onset of atrial fibrillation (AF) episodes. This PWMV is hypothesized to be an index of vulnerable atrial substrate, allowing to identify instability increases preceding the AF episode onset. We analyzed 32 ambulatory ECG recordings from subjects with paroxysmal AF. For each i-th subject and j-th AF episode, the PWMV was characterized in consecutive 2-min windows ($k = 1 \dots 30$) within the last 60 min before the AF onset. For each 2-min window, the median absolute deviation (MAD) of the P wave signals $p_{\mathrm{MAD}}^{i,j,k}(n)$; and the MAD energy normalized to the median of the P wave energy in each subject $E_r^{i,j}(k)$ were measured. Then, for each subject, a normalized median across AF episodes was obtained, $\tilde{E}_r^i(k)$. A two-segment linear function fit of $\tilde{E}_r(k)$ temporal evolution, by least squares error (LSE) minimization was used to characterize the cohort dynamics. Analyzing the cohort dynamics of $\tilde{E}_r(k)$, a relative stability can be observed up to 8 minutes before the AF episode onset, when $\tilde{E}_r(k)$ value starts increasing. In conclusion, PWMV can be monitored by quantifying the P-wave short-time MAD relative energy, which shows an increasing trend within the 8 minutes previous to the AF onset.

1. Introduction

Atrial fibrillation (AF) is one of the most common cardiac arrhythmias that is associated with a variety of potential complications. Projections indicate an escalation in the incidence and prevalence of this disease in forthcoming years [1]. The presence of AF is associated with an increased risk of mortality, as well as with a 4- to 5-fold higher risk of stroke [2]. These factors represent a significant healthcare burden. It is therefore evident that timely diagnosis and prediction of AF incidence can help in allocating valuable healthcare resources to those most in need, thereby significantly enhancing the effectiveness of prevention strategies.

Surface ECG provides critical insights into the electrical and structural properties of the atria, particularly evident in P-waves [3]. This information is crucial to identify patients who currently have AF episodes or those at high risk of developing AF in the near future [4, 5]. Short-term P-wave morphological variability (PWMV) has been shown to be a marker of atrial electrical instability and may reflect instabilities that precede AF [6–8]. The present study aims to analyze the temporal evolution of PWMV within the hour preceding the onset of AF episodes and to identify when noticeable PWMV changes start to occur before an AF episode.

2. Materials and Methods

2.1. Data Set

The study database, SPAFDB, contains 36 ambulatory Holter ECG recordings from patients diagnosed with paroxysmal AF (mean[range] recording duration: 104[21–156] hours) [9]. One of the recordings was excluded from the analysis due to the absence of usable AF annotations. Two additional recordings were discarded due to suboptimal signal quality, and another was omitted since it did not have any one-hour sinus rhythm segment preceding AF onset. Consequently, a total of 32 recordings were subjected to analysis. Twenty-nine of the analyzed recordings contained 3 leads sampled at 257 Hz, while the remaining three recordings contained 12 leads sampled at 250 Hz. The specific lead configuration for the 3 lead

recordings is unknown. All ECGs were resampled to 500 Hz and, for the 12-lead recording, only leads I, II and III were considered for the analysis.

2.2. ECG Preprocessing and Segmentation

The ECG preprocessing comprised two stages: First, power line interference and muscle noise were attenuated using a 6th-order Butterworth low-pass filter with cut-off frequency of 40 Hz. Subsequently, baseline wander was filtered using 6th order Butterworth high-pass filter with cut-off frequency of 0.5 Hz.

Multilead QRS detection was performed by a wavelet-based detector [10], and AF episodes were annotated using an AF detector based on fuzzy logic [11], with posterior manual verification by an AF specialist to complete the annotation process.

All available 60-minute segments immediately preceding the onset of an AF episode were selected. All AF episodes without at least one hour of prior sinus rhythm were excluded from the analysis.

2.3. Spatio-Temporal PCA-Based Lead Transformation for P-Wave Enhancement

To improve the signal-to-noise ratio (SNR) and thus enhance the P-wave's morphological features, we applied a linear spatial lead transformation based on Principal Component Analysis (PCA) to the three ECG leads, using the methodology described in [12–14]. The method operates in two stages: (1) PCA transformation parameter (basis) learning performed in a subset of the ECG segmented P waves within each ECG segment, and (2) spatial projection of the ECG signal onto the derived PCA basis.

1) PCA Basis Learning

Each one-hour segment under analysis is expressed in vector notation as $\mathbf{x}_l = [x_l(0), \cdots, x_l(M-1)]$, with the three leads piled together in the matrix $\mathbf{X} = [\mathbf{x}_1^T, x_2^T, \mathbf{x}_3^T]^T$, with $M = 1,800,000$ the total number of samples in the segment.

At each j-th one-hour ECG segment, 60 individual P waves, starting 60 seconds after the beginning of the segment, were segmented using a 140-ms window starting 220 ms before the QRS fiducial point, thus guaranteeing that the P waves are completely included within them. For each q-th beat, the segmented P wave is $\mathbf{p}_{l,q} = [p_{l,q}(0), \cdots, p_{l,q}(N-1)]^T$, where $N = 70$ is the number of samples in the P-wave window and $q \in \{1, 2, ..., Q = 60\}$. By combining the P-waves in the 3 leads, we obtain the matrix

$$\mathbf{P}_q = [\mathbf{p}_{1,q}, \mathbf{p}_{2,q}, \mathbf{p}_{3,q}]^T \tag{1}$$

for the q-th beat.

The n-th column of $\mathbf{P}_q$ contains the voltage of all 3 leads at sample n of the q-th beat. The P wave data matrix $\mathbf{P}$ was then created by concatenating the $\mathbf{P}_q$ matrices for the 60 beats:

$$\mathbf{P} = [\mathbf{P}_1, \mathbf{P}_2, ..., \mathbf{P}_Q]^T. \tag{2}$$

The spatial correlation matrix $\mathbf{R_P}$ of $\mathbf{P}$ was estimated as:

$$\widehat{\mathbf{R}}_{\mathbf{P}} = \frac{1}{QN}\mathbf{P}\mathbf{P}^T. \tag{3}$$

The set of principal components was obtained by solving the eigenvector equation for $\widehat{\mathbf{R}}_{\mathbf{P}}$ [12]:

$$\widehat{\mathbf{R}}_{\mathbf{P}}\mathbf{\Psi} = \mathbf{\Psi}\mathbf{\Lambda} \tag{4}$$

where $\mathbf{\Lambda}$ is the eigenvalue diagonal matrix with the eigenvalues sorted in descending value order and $\mathbf{\Psi}$ contains in each column the eigenvectors defining the PCA.

2) ECG Signal Projection

The three-lead ECG signals $\mathbf{X}$ were projected into the space defined by the derived PCA basis $\mathbf{\Psi}$ using:

$$\mathbf{Y} = \mathbf{\Psi}^T\mathbf{X}. \tag{5}$$

Given that the basis $\mathbf{\Psi}$ was exclusively trained in P-waves segments, the first component, $\mathbf{y}_1 = [y_1(0), \cdots, y_1(M-1)]$, of $\mathbf{Y}$ is expected to capture the majority of the energy, and presumably variability, associated with P-wave morphology.

2.4. P-Wave Morphological Variability

After the PCA transformation, the P-wave morphological variability is analyzed in the first transformed lead of $\mathbf{Y}$. The subsequent analyses are applied on $\mathbf{y}_1$ lead (the first principal component).

The P waves $p_q^{i,j,k}(n)$ are segmented following the same procedure detailed in Section 2.3. QRS fiducial points in $\mathbf{y}_1$ were detected using the wavelet-based delineator [10].

For each i-th subject and j-th AF episode, the one-hour, pre-AF PWMV is characterized in all the k-th consecutive 2-min windows, $k \in \{1, \cdots, K = 30\}$, as:

1) The median absolute deviation (MAD) of the q-th beat P waves $p_q^{i,j,k}(n)$, is defined as:

$$p_{\mathrm{MAD}}^{i,j,k}(n) = \underset{q}{\mathrm{mad}}\left\{p_q^{i,j,k}(n)\right\}. \tag{6}$$

2) The energy of $p_{\mathrm{MAD}}^{i,j,k}(n)$ normalized by the median of the P wave energy in each subject ($E_{P_{\mathrm{med}}}^i$), computed as:

$$E_r^{i,j}(k) = \frac{\sum_{n=1}^{N}\left(p_{\mathrm{MAD}}^{i,j,k}(n)\right)^2}{E_{P_{\mathrm{med}}}^i}, \tag{7}$$

where $E^i_{P_{\text{med}}}$ is estimated as:

$$E^i_{P_{\text{med}}} = \underset{j,k,q}{\text{med}} \left\{ \sum_{n=1}^{N} \left(p_q^{i,j,k}(n) \right)^2 \right\}. \quad (8)$$

This normalization by $E^i_{P_{\text{med}}}$ removes amplitude-dependent biases in PWMV measurements.

3) Patient-specific $E^i_r(k)$ patterns were evaluated by calculating median values across all AF episodes for each subject:

$$E^i_r(k) = \underset{j}{\text{med}}\{E^{i,j}_r(k)\} \quad (9)$$

Patient specific normalization of each $E^i_r(k)$ series is done using the patient median value during the initial 10-minute reference period ($k \in [1, 5]$) to isolate temporal PWMV dynamics from inter-subject amplitude variations, thus enabling cohort-level comparative analysis.

$$\tilde{E}^i_r(k) = \frac{E^i_r(k)}{\underset{k\in[1,5]}{\text{med}} \{E^i_r(k)\}} \quad (10)$$

Finally, the dynamics of the P wave morphological variability (PWMV) of the cohort was characterized by computing the median across all patients
A two-segment least-squares linear function fit to the median $E_r(k)$ series in the cohort is used to characterize the cohort dynamics.

3. Results and Discussion

P-wave ensemble construction (Fig. 1) demonstrates variable morphological variability across two-minute segments of recording #2. The $p^{i,j,k}_{\text{MAD}}(n)$ in the Figure values reflects well ensemble dispersion.

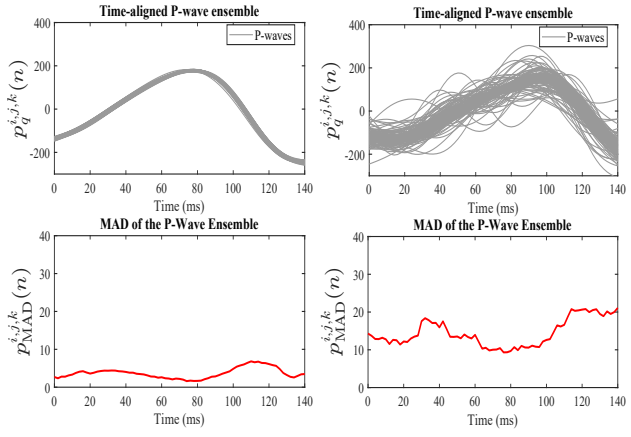

Figure 1: *Two-minute segment P-wave ensemble and its corresponding $p^{i,j,k}_{\text{MAD}}(n)$ (Recording # 2). (a) A P-wave ensemble with low-variability, (b) A P-wave ensemble with high-variability.*

In 56% of patients, the highest values of $E^i_r(k)$ were observed in the last 30 minutes before the AF event, occasionally exceeding twice the mean of $E^i_r(k)$. Fig. 2 shows the distribution of $\tilde{E}^i_r(k)$ values in the hour before AF onset in the 32-patient cohort. Both the median and dispersion of $\tilde{E}^i_r(k)$ values exhibit an upward trend when approaching the event, suggesting increased P-wave variability in the last minutes before Af onset. This pattern may indicate a progressive deterioration in the electrical organization of the atrium before the AF onset.

The distribution of $\tilde{E}^i_r(k)$ at each temporal window was compared against that of the initial window (-60 to -58 min before the AF onset), by the Wilcoxon signed-rank test for paired samples with p-values <0.05 being considered significant. This methodology identifies the point at which P-wave dynamics deviate significantly from the baseline. The Wilcoxon test identified statistically significant differences exclusively in the final two pre-event windows: -4 to -2 minutes ($p = 0.036$) and -2 to 0 minutes ($p = 0.004$). These results demonstrate a significant increase in P-wave variability energy during the terminal pre-AF phase, supporting the hypothesis of accelerated atrial electrical destabilization immediately preceding AF onset.

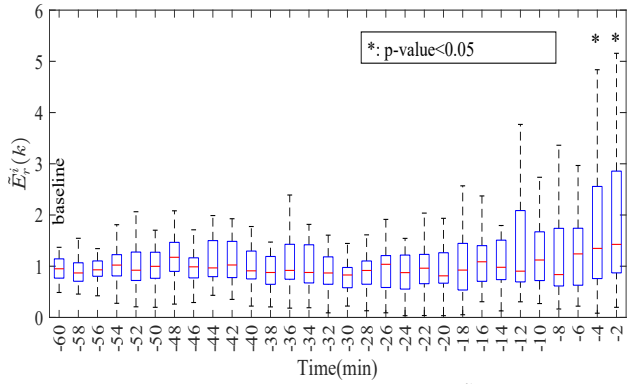

Figure 2: *Patient-specific temporal distribution of $\tilde{E}^i_r(k)$. Statistically significant different distributions (Wilcoxon test, $p < 0.05$) relative to the ones at reference baseline (-60 to -58 min) are indicated by (*).*

Fig. 3 illustrates the temporal dynamics of $\tilde{E}_r(k)$ (corresponding to the median values in Fig. 2) during the pre-AF period. The analysis reveals two different trends: (1) an initial relatively stable period (from minute -60 to approximately minute -8) with minimal $\tilde{E}_r(k)$ fluctuations, followed by (2) a sustained increase beginning at minute -8 until AF onset. This transition point marks a fundamental shift in P-wave dynamics, characterized by progressively increasing $\tilde{E}_r(k)$ values that hypothetically reflects deterioration of atrial electrical organization preceding AF initiation. These observations align with the statistical significance patterns demonstrated in Fig. 2.

These results support the hypothesis that PWMV remains relatively stable during periods distant from AF

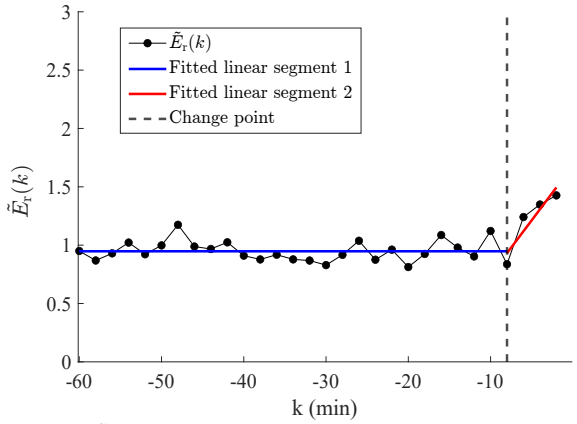

Figure 3: $\tilde{E}_r(k)$ *and its two fitted linear segments. PWMV increase turning point is indicated by a dashed line*

events but exhibits an abrupt intensification during the final minutes preceding AF onset. This temporal pattern may have significant implications for short-term impending arrhythmia prediction, suggesting that MAD energy accurately captures pre-AF PWMV dynamics and could serve as a novel AF risk biomarker.

4. Conclusion

P-wave morphological variability can be monitored by quantifying their short-time MAD relative and subject normalized energy, showing an increasing P-wave morphological variability trend in the last 8 minutes before AF onset.

Acknowledgments

This work was supported by the European Union's Horizon Europe programme under the Marie Skłodowska-Curie GA No:101150167 -MESMODI-BCG- and under project PID2022-140556OB-I00 from MICIN, and ARAID from Aragon Goverment, Spain.

References

[1] Colilla S, Crow A, Petkun W, Singer DE, Simon T, Liu X. Estimates of current and future incidence and prevalence of atrial fibrillation in the u.s. adult population. The American Journal of Cardiology 2013;112(8):1142–1147. ISSN 0002-9149.

[2] Harrison SL, Fazio-Eynullayeva E, Lane DA, Underhill P, Lip GYH. Atrial fibrillation and the risk of 30-day incident thromboembolic events, and mortality in adults $\geq$ 50 years with covid-19. Journal of Arrhythmia 2021;37(1):231–237.

[3] German DM, Kabir MM, Dewland TA, Henrikson CA, Tereshchenko LG. Atrial fibrillation predictors: Importance of the electrocardiogram. Annals of Noninvasive Electrocardiology 2016;21(1):20–29.

[4] Giannopoulos G, Tachmatzidis D, Moysidis DV, Filos D, Petridou M, Chouvarda I, Vassilikos VP. P-wave indices as predictors of atrial fibrillation: The lion from a claw. Current Problems in Cardiology 2024;49(1, Part A):102051. ISSN 0146-2806.

[5] Tachmatzidis D, Tsarouchas A, Mouselimis D, Filos D, Antoniadis AP, Lysitsas DN, Mezilis N, Sakellaropoulou A, Giannopoulos G, Bakogiannis C, Triantafyllou K, Fragakis N, Letsas KP, Asvestas D, Efremidis M, Lazaridis C, Chouvarda I, Vassilikos VP. P-wave beat-to-beat analysis to predict atrial fibrillation recurrence after catheter ablation. Diagnostics 2022;12(4). ISSN 2075-4418.

[6] Tzou HA, Lin SF, Chen PS. Paroxysmal atrial fibrillation prediction based on morphological variant p-wave analysis with wideband ecg and deep learning. Computer Methods and Programs in Biomedicine 2021;211:106396. ISSN 0169-2607.

[7] Filos D, Chouvarda I, Tachmatzidis D, Vassilikos V, Maglaveras N. Beat-to-beat p-wave morphology as a predictor of paroxysmal atrial fibrillation. Computer Methods and Programs in Biomedicine 2017;151:111–121. ISSN 0169-2607.

[8] Conte G, Luca A, Yazdani S, Caputo ML, Regoli F, Moccetti T, Kappenberger L, Vesin JM, Auricchio A. Usefulness of p-wave duration and morphologic variability to identify patients prone to paroxysmal atrial fibrillation. The American Journal of Cardiology 2017;119(2):275–279. ISSN 0002-9149.

[9] Henriksson M, Martín-Yebra A, Butkuvienė M, Rasmussen JG, Marozas V, Petrėnas A, Savelev A, Platonov PG, Sörnmo L. Modeling and estimation of temporal episode patterns in paroxysmal atrial fibrillation. IEEE Transactions on Biomedical Engineering 2021;68(1):319–329.

[10] Martínez J, Almeida R, Olmos S, Rocha A, Laguna P. A wavelet-based ecg delineator: evaluation on standard databases. IEEE Transactions on Biomedical Engineering 2004;51(4):570–581.

[11] Petrėnas A, Sörnmo L, Lukoševičius A, Marozas V. Detection of occult paroxysmal atrial fibrillation. Medical Biological Engineering Computing 2015;53:287–297. ISSN 1741-0444.

[12] Castells F, Laguna P, Sörnmo L, Bollmann A, Roig JM. Principal component analysis in ecg signal processing. EURASIP Journal on Advances in Signal Processing 2007; 2007:074580. ISSN 1687-6180.

[13] Moreno C, Martín-Yebra A, Savelev A, Platonov P, Laguna P, Martínez JP. Analysis of p-wave changes for prediction of atrial fibrillation episodes. In 2022 Computing in Cardiology (CinC), volume 498. 2022; 1–4.

[14] Monasterio V, Laguna P, Martínez JP. Multilead analysis of t-wave alternans in the ecg using principal component analysis. IEEE Transactions on Biomedical Engineering 2009; 56(7):1880–1890.

Address for correspondence:

Maikel Noriega
Campus Río Ebro. Mariano Esquillor, S/N.50018 Zaragoza,Spain
mnoriega@unizar.es